Fall 2019

Near-field scanning based shielding effectiveness extraction for board level shielding cans

Harsh Shrivastav

Department:

NEAR-FIELD SCANNING BASED SHIELDING EFFECTIVENESS EXTRACTION FOR BOARD LEVEL SHIELDING CANS

by

HARSH SHRIVASTAV

A THESIS

Presented to the Faculty of the Graduate School of the

MISSOURI UNIVERSITY OF SCIENCE AND TECHNOLOGY

In Partial Fulfillment of the Requirements for the Degree

MASTER IN SCIENCE

in

ELECTRICAL ENGINEERING

2019

Approved by:

Dr. Chulsoon Hwang, Advisor
Dr. Daryl Beetner
Dr. Jun Fan

PUBLICATION THESIS OPTION

This thesis consists of the following article, formatted in the style used by the Missouri University of Science and Technology:

Paper I: Pages 2-32; Near Field Scanning based Shielding Effectiveness Extraction for Board Level Shielding Cans, has been submitted to IEEE Transactions on Electromagnetic Compatibility.

ABSTRACT

The conventional definition of shielding effectiveness is well suited for calculating electromagnetic shielding in the far-field. However, in the near field, shielding effectiveness calculation is not so straight forward. In radio frequency interference problems, most of the field coupling occurs in near field. Having a well-defined method to calculate near-field shielding effectiveness is important for estimating the suppression of radio frequency interference using the shield cans. In this research, a method to extract the shielding effectiveness of board level shielding cans using near field scanning is developed. Shielding effectiveness is defined by modelling the shielded noise source as equivalent dipole moments. Accuracy of the equivalent source is analyzed by using least square error and correlation coefficient as confidence check parameters. Applying reciprocity theorem, the voltage coupled on a PIFA antenna from an unshielded and a shielded source is calculated. Coupled voltage from a shielded noise source serves as the reference and is used to validate the effectiveness of the developed method. Practical shield cans were used to study and develop the shielding effectiveness extraction method using full wave 3D simulations.

ACKNOWLEDGMENTS

I would like to express my gratitude to my graduate advisor, Dr. Chulsoon Hwang, for his expert guidance and valuable insight for my research work. I am grateful to him for his constant support and encouragement throughout my graduate program. I would like to thank Dr. David Pommerenke for his criticisms and support, without which I wouldn't have passed many hurdles during my work at "Electromagnetic Compatibility Laboratory", at Missouri S&T. I also thank Dr. Daryl Beetner and Dr. Jun Fan for being a part of my thesis committee and putting in time to review this research work.

A special thanks to all my friends for providing their support and helping me during the tough times. Finally, I thank my parents, sister and entire family for their unconditional love and emotional support throughout my education at Missouri S&T.

TABLE OF CONTENTS

Page

SECTION

LIST OF ILLUSTRATIONS

PAPER I Page

SECTION

LIST OF TABLES

PAPER I Page

SECTION

SECTION

1. INTRODUCTION

"A system is electromagnetically compatible with its environment if it does not interfere with components in its environment and if it is not susceptible to electromagnetic energy within its environment" [1]. Modern electronic devices such as smartphones, tablets, smart home appliances are densely populated with integrated circuits (ICs), RF antennas and power management ICs. High speed digital circuits, if not properly designed and routed can easily couple to nearby components, causing radio frequency interference issues within the device. Shielding enclosures are often used to suppress/prevent such interference problems. These enclosures also reduce the susceptibility of a device to the surrounding electromagnetic energy.

Calculation and measurement of shielding effectiveness is well defined in far-field. However, in near field, shielding effectiveness calculation is not so simple. This is because, assumptions made for calculating far-field shielding effectiveness no longer remain true in near field [1]. In this research, a method to extract near field shielding effectiveness of board level shielding cans using near field scanning is developed. Unshielded and shielded source are modelled using equivalent magnetic dipole moments. Two confidence check parameters are applied to check the accuracy with which source can be modelled using the equivalent magnetic dipole moments. Developed shielding effectiveness extraction method is validated using measurements and 3D simulations.

PAPER

I. NEAR FIELD SCANNING BASED SHIELDING EFFECTIVENESS EXTRACTION FOR BOARD LEVEL SHIELDING CANS

H. Shrivastav, C. Hwang

Department of Electrical and Computer Engineering, Missouri University of Science and Technology, Rolla, MO 65409

ABSTRACT

The conventional definition of shielding effectiveness is well suited for calculating electromagnetic shielding in the far-field. However, in the near field, shielding effectiveness calculation is not so straight forward. In radio frequency interference problems, most of the field coupling occurs in near field. Having a well-defined method to calculate near-field shielding effectiveness is important for estimating the suppression of radio frequency interference using the shield cans. In this paper, a method to extract the shielding effectiveness of board level shielding cans using near field scanning is developed. Shielding effectiveness is defined by modelling the shielded noise source as equivalent dipole moments. Accuracy of the equivalent source is analyzed by using least square error and correlation coefficient as confidence check parameters. Applying reciprocity theorem of electromagnetics, the voltage coupled on a PIFA antenna from an unshielded and a shielded source is calculated. Coupled voltage from a shielded noise source serves as the reference and is used to validate the effectiveness of the developed method. Practical shield cans were used to study and develop the shielding effectiveness extraction method using full wave 3D simulations.

1. INTRODUCTION

With advancements in science and technology, modern electronic devices have become quite capable in establishing high speed wireless connections. For example, a smartphone can wirelessly connect to a smart television, a smart watch, a smart home appliance, or a smart audio speaker. Such connectivity is attributed to the presence of receiving/transmitting radio frequency (RF) antennas. A typical smartphone has antennas for Wi-Fi, Bluetooth, global positioning system (GPS), near-field communication (NFC) and various cellular bands. These RF antennas are present alongside high-speed digital clocks, processors, power management integrated circuits (ICs), and differential data channels. High speed digital circuits, if not properly designed and routed, can easily couple to nearby RF antennas, causing radio receiver desensitization. To prevent radio frequency interference (RFI) and desense problems, the use of well-designed shielding cans with accurately known values of shielding effectiveness is important. General design rules, such as providing a good signal return path, keeping the potential noise sources away from large metal structures, and reducing the length of transmission lines, are more and more difficult to meet with the increased demand for integration. Shielding enclosures are therefore often employed to reduce interference from noise sources.

Shielding effectiveness (SE) of an enclosure is typically defined as the ratio of incident field on the enclosure to the transmitted field through the enclosure. This definition is based on the assumption that the incident electromagnetic (EM) wave is a uniform plane wave, with E- and H- fields in the far-field region. Radiated EM fields can be thoroughly measured using an anechoic chamber. A measurement antenna can be put into the chamber

to measure the intensity of the electromagnetic field radiated by the shielded source and then contrasted with that measured by the antenna without the shield. Using the conventional definition, far-field SE can be calculated efficiently and accurately [1]. However, in the near field, the assumption that the EM wave behaves as a uniform plane wave no longer remains true. Furthermore, the impedance of the wave changes with the type of the source producing the field [2]. This makes calculation of near field SE complicated. In RFI problems, most of the field coupling occur in the near field. Having a well-defined method to calculate near field SE is critical for quantifying reduction in RFI using shielding cans.

With ongoing research, a few methods to define and measure near field SE have been developed. Gao et al. [3] defined SE of system-in-package (SiP) module based on the spatial average value of the radiated magnetic near field from the SiP module. The definition of SE was validated by correlating far-field SE extracted using a reverberation chamber with measured near field SE. Kim et al. [4] proposed two new IC-stripline designs for measuring near field SE of on-board metallic cans. Although [3]-[4] presented a way to measure near-field SE, they failed to provide insight into the impact of measured SE on the coupling between a shielded source and victim circuit. Also, the shielding cans used for analysis in [3]-[4] were ideal, as they formed a complete faraday cage around the source. Practical shielding cans have ventilation slots and castellated edges for thermal relief and reflow soldering. Slots and castellation gaps with dimensions larger than $\lambda/10$ at frequencies of interest are capable of acting as antennas [5], which changes the emission characteristics of the source underneath the shield. This means that at the resonant frequency of the slot antenna, SE of the metallic can will be relatively lower than SE at

non-resonant frequencies. Therefore, SE must be extracted by considering radiation from slots on the shielding enclosure. Hwang et al. [6] proposed a definition of SE using equivalent dipole moments, which were extracted using the transverse electromagnetic (TEM) cell method. Although [6] considered radiation from slots on the shielding can, it suffers from the limitation that the shielded source must be placed at the center of TEM cell. For a practical device, such as a cell phone, it is not always possible to keep the shielded source at the center of the TEM cell. Moreover, there might be several sources in a real product. Exciting only one shielded source for measuring SE might prove to be a challenge. This makes [6] of limited use for real products.

In this paper, a new method to extract SE of board level shielding cans using near field scanning is proposed. SE is defined by reconstructing the shielded source using equivalent dipole moments, which are extracted using near field data from the shielded source. Use of near field data allows for accounting of changes in radiation characteristics of the source due to slots, castellations, and dimensions of the shield can. When multiple sources are present, near field scanning can be used to focus on a specific shielded source and obtain field data for application of the proposed method. An analytical equation to estimate voltage coupled on a RF antenna using the extracted shielding effectiveness is also formulated. Proposed method and formulations are validated through full wave 3D simulations.

2. RFI SIMULATION WITH SHIELDED SOURCE

A typical RFI problem is illustrated in Figure 1. An active IC and a shielded IC are coupling to an RF antenna in the near field, causing RFI. By analyzing the coupled voltage from the shielded source to the victim antenna, suppression of RFI with a shielding can is studied. All the calculations are performed using full wave simulations.

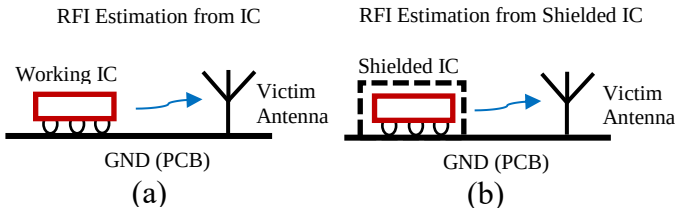

Figure 1. RFI characterization. (a) From an active IC. (b) From a shielded IC.

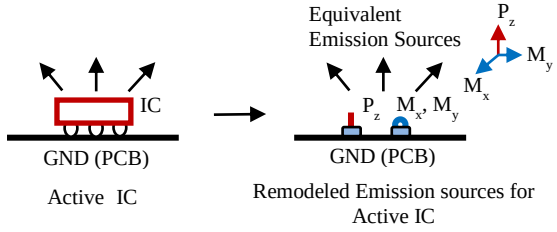

Figure 2. Equivalent dipole moments model of an active IC.

Using multipole expansion theory [7], any arbitrary electrically small source can be modelled using a set of electric and magnetic dipole moments. The source is replaced with a set of appropriate electric dipoles P_x, P_y, P_z and magnetic dipoles M_x, M_y, M_z in Cartesian coordinates. Through [7] - [9], an active IC located above an infinitely large ground plane can be modelled using equivalent dipole moments (P_z, M_x, and M_y). Figure 2 shows a representation of an active IC with equivalent dipole moments. In this study, a

magnetic dipole pointing in the x direction (M_x dipole) is used to approximate noise from a working IC. RFI is expressed as the amount of voltage coupled from the source to the victim antenna, with the victim antenna terminated with 50 Ω.

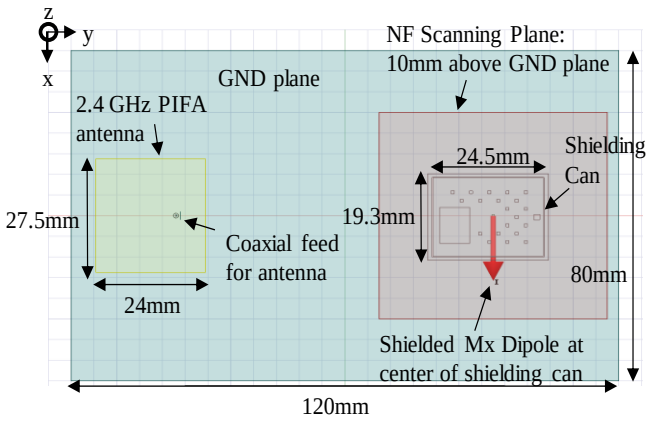

Figure 3. Simulation model for estimating RFI and SE with shielded M_x dipole.

The electromagnetic field coupling from an M_x dipole and a shielded M_x dipole to a victim 2.4 GHz PIFA antenna is evaluated by designing a simulation model in ANSYS HFSS [10]. Strength of the M_x dipole is kept as 1 Vm and the frequency range for simulation is from 500 MHz – 6 GHz. The simulation model for calculating coupled voltage from the shielded M_x dipole is shown in Figure 3. Voltage coupled to the PIFA antenna can be calculated by integrating E-field along a tangential line connecting the signal and signal return conductor on the coaxial feed of the antenna.

Coupled voltage on PIFA antenna from the single M_x dipole and shielded M_x dipole is shown in Figure 4. For both cases, maximum voltage is coupled at the resonant frequency of the antenna i.e. 2.4 GHz. The difference between the coupled voltage from a single M_x dipole and a shielded M_x dipole represents the suppression of RFI from the shielding can.

In other words, the difference represents shielding effectiveness of the shielding can. In section 4, coupled voltage will be estimated using an analytical equation derived from the dipole moments-based reciprocity method [11]-[12]. Using the derived analytical equation, the proposed SE extraction method will be validated.

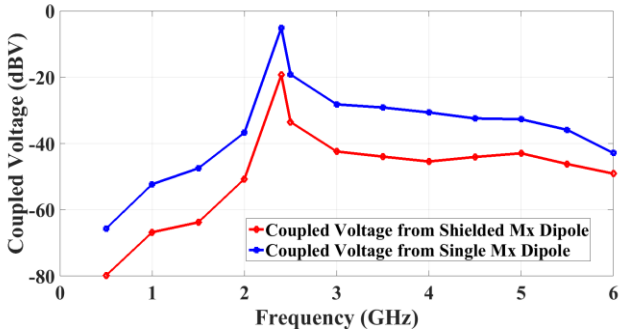

Figure 4. Coupled voltage comparison between single M_x dipole and shielded M_x dipole.

3. NEAR FIELD SCANNING BASED SE EXTRACTION

3.1. SHIELDING EFFECTIVENESS AND RFI DEFINITION

Similar to an IC, a small shielding can enclosing an IC can also be modelled using equivalent dipole moments by applying the physics and equations as mentioned in [6]-[9]. It is worth mentioning that RFI and desense issues caused by the source behaving as a single dipole have been reported in many research papers [13]-[15]. Therefore, it is reasonable to assume that a single M_x dipole can represent an IC. With this assumption, a shielded M_x dipole can be modelled using equivalent dipole moments as follows.

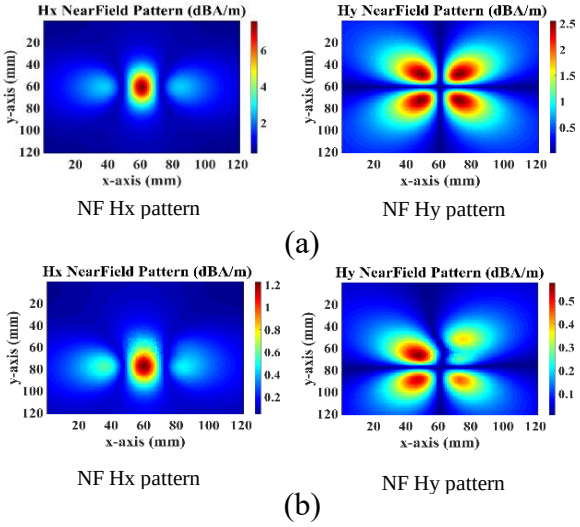

Figure 5. Nearfield patterns at scan height of 10mm. (a) Nearfield patterns from single M_x dipole. (b) Nearfield patterns from shielded M_x dipole.

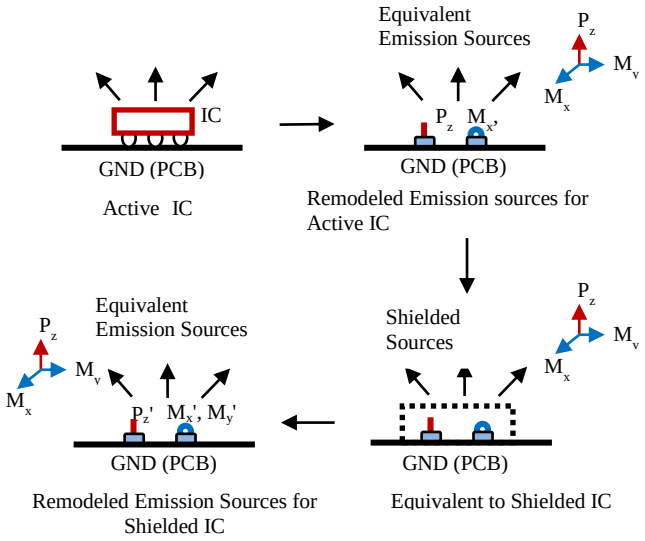

Figure 6. Dipole moment representation of active IC and shielded IC.

Near field patterns measured above a single M_x dipole and shielded M_x dipole at a frequency of 2.4 GHz and scan height of 10 mm are illustrated in Figure 5. Design and geometrical details of the simulation model used to obtain the near field pattern from

shielded M_x dipole is shown in Figure 3. The strength of M_x dipole is kept as 1 Vm. By comparing the near field H_x and H_y patterns shown in Figure 5, it is evident that these patterns approximately match with each other. Slight distortion in the shape of the near field H_y pattern in Figure 5(b) is due to the geometry of the shielding can used. Owing to the similarity in the shape of the near field patterns, it is possible to model the shielding can enclosing an M_x dipole in terms of equivalent dipole moments (P_z', M_x', and M_y'). Workflow for modelling an active IC and shielded IC with dipole moments is shown in Figure 6.

When a source is shielded with an enclosure, the electric field generated by the source gets capacitively coupled with the body of the enclosure, resulting in surface currents. Magnetic field generated by the source produces eddy currents on the surface of the shield. If the shield is several skin depths thick at the frequency of interest, eddy currents generate an opposing magnetic field, which cancels the magnetic field generated by the source. However, skin depth varies inversely with the square root of frequency. This means, at frequencies where skin depth is comparable to the thickness of the shield, cancellation of source magnetic field would not be very effective and there will be leakage of magnetic field through the shield. Surface currents due to electric field coupling do not get cancelled. Instead, they look for the path of least impedance to return to the source. Slots on the body of the shield create distortion in the path of surface currents, resulting in noise voltage across the slots. Depending on the wavelength at the frequency of operation and dimensions of apertures on the shield, developed noise voltage can act as an excitation source for the unintentional antenna created by slots on the shield. If the dimension of a slot is greater than $\lambda/10$ at the frequency of interest, it acts as an efficient antenna [5].

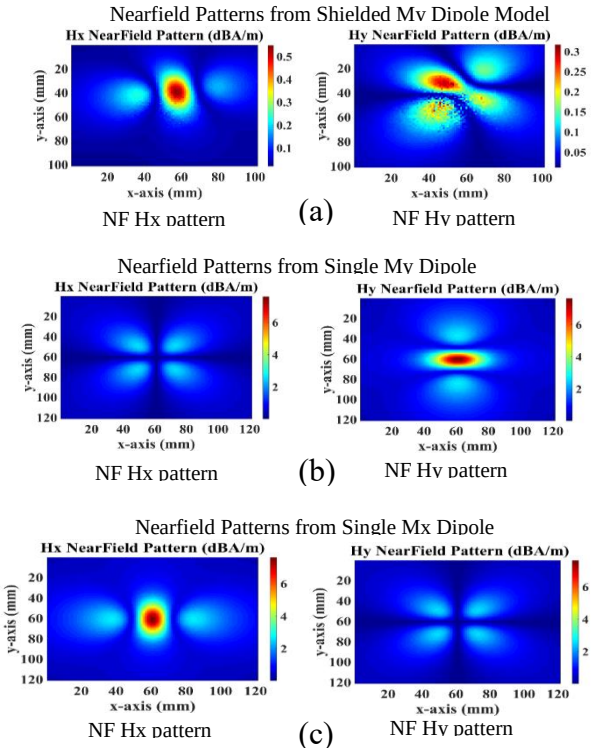

Figure 7. Nearfield patterns comparison for analysis of equivalent source transformation. (a) Nearfield patterns from shielded M_y dipole. (b) Nearfield patterns from single M_y dipole. (c) Nearfield patterns from single M_x dipole.

Of course, slots with dimensions smaller than $\lambda/10$ can also act as antennas and leak EM waves, but their impact on SE would be much less than the impact of radiation from slots larger than $\lambda/10$. The combined effect of EM radiation from source and slot antennas results in a change in the radiation characteristics of the original source, causing equivalent source transformation. This means a shielded M_x dipole could undergo equivalent source transformation to act as an M_y dipole. Therefore, from an RFI point of view, SE must be calculated by taking into account the phenomenon of equivalent source transformation. An example of equivalent source transformation is illustrated in Figure 7. By analyzing the H_x and H_y near field patterns in Figure 7, it is apparent that shielded M_y dipole has

undergone equivalent source transformation and is now acting as a single M_x dipole instead of a single M_y dipole.

Equivalent dipole moments for a shielded source embody the physics of equivalent source transformation. Thus, using equivalent dipole moments, SE is defined as [6]:

$$SE_{S_i S_j} = \frac{S_i}{S'_j} \tag{1}$$

where, $S_i = P_z,\ jk_0 M_x,$ or $jk_0 M_y$

$S'_j = P'_z,\ jk_0 M'_x,$ or $jk_0 M'_y$

S_i represents dipole moments for an IC whereas S'_j represents equivalent dipole moments for a shielded IC. k_0 is the free space wave number. The term jk_0 has been introduced to make SE a unitless quantity. Subscripted *SE* represents the shielding effectiveness value for the dipole component, which was created from the original dipole source due to equivalent source transformation. For example, SE_{PzMx} represents SE for an equivalent M_x dipole when a P_z dipole is used as an excitation source.

$$SE_{PzMx} = P_z \,/\, jk_0 M'_x \tag{2}$$

With source and shielded source modelled as dipole moments, RFI from dipole moment to victim antenna can be calculated by applying the reciprocity theorem of electromagnetics [16]. Following the derivation in [17], the coupled voltage, $V_{coupled}$, can be analytically calculated as:

$$V_{coupled} = TF\left(-\vec{E}_{z,rev} \cdot \vec{P}_z + \vec{H}_{x,rev} \cdot \vec{M}_x + \vec{H}_{y,rev} \cdot \vec{M}_y\right) \tag{3}$$

where, $H_{x,rev}$, $H_{y,rev}$ are the x and y magnetic field components at the location of the dipole when the victim antenna is excited, $E_{z,rev}$ is the z component of electric field at the dipole

location in the reverse problem, P_z is the electric dipole moment in the z direction and M_x, M_y are magnetic dipole moments pointing in the x and y directions, respectively. Depending on the type of dipole moment representing the source, (3) can be simplified. For example, if an M_x dipole is used to represent the source, then coupled voltage will be calculated as:

$$V_{coupled} = TF\left(\overrightarrow{H}_{x,rev} \cdot \overrightarrow{M}_x\right) \tag{4}$$

Equation (3) embodies the physics for calculating coupled voltage on a victim antenna with dipole moments as the aggressor. Using the proposed definition of SE in (1) and the dipole moments-based reciprocity method [11]-[14], coupled voltage to an antenna from a single M_x dipole (source) and shielded M_x dipole (shielded source) can be calculated as:

$$V_{coupled,1} = S_i \times TF \tag{5}$$

$$V_{coupled,2} = S_j' \times TF \tag{6}$$

where, $V_{coupled,1}$ represents coupled voltage from a single M_x dipole. $V_{coupled,2}$ represents the coupled voltage from a shielded M_x dipole. S_i is the dipole moment value of a single M_x dipole. S_j' represents the dipole moment value of an equivalent dipole representing the shielded M_x dipole. *TF* is the transfer function between the reverse fields measured at the location of the equivalent dipole in the reverse problem and the incident voltage used to excite the antenna [11]-[14].

$$TF = \frac{Z_L}{2V_{rev}^+} H_i \tag{7}$$

where, Z_L represents 50 Ω termination for the victim antenna in the forward problem. H_i is the reverse H-field measured at the location of equivalent dipole moment. represents the incident voltage excitation used to excite the antenna in the reverse problem. Through (1), (3), (5)-(7), $V_{coupled,2}$ can be rewritten as:

$$V_{coupled,2} = \frac{S_i}{SE} \times TF \tag{8}$$

Using (8), extracted SE obtained from the proposed method can be applied to estimate voltage coupled on an antenna with a shielded source.

3.2. EQUIVALENT DIPOLE MOMENTS EXTRACTION

Accurately extracting dipole moments corresponding to an IC and a shielded IC are critical for calculating SE using (1). Assuming, an IC shielded with an enclosure could be modelled using equivalent dipole moments, previously, dipole moment extraction was done using the TEM cell method [6],[18]. For the TEM cell method to work efficiently, the DUT must be placed at the center of the TEM cell. In a real product, there might be several potential sources which will require shielding. Fixing each source at the center of the TEM cell facing towards the septum is not possible. Furthermore, exciting only a specific shielded source for extracting equivalent dipole moments will also not be feasible. Due to these limitations, extraction of equivalent dipole moments using a TEM cell is of limited use in a real product.

To overcome the drawbacks of the TEM cell method, the near field scanning based source reconstruction method is applied in this paper for extraction of equivalent dipole moments. Tangential fields on the near field scanning plane above the shielded source are

used to calculate equivalent dipole moments. The optimal location for an equivalent source is obtained by using measured H_x and H_y near field patterns. Any change in the radiation characteristics of the shielded source or offset in location of the equivalent dipole moment due to design and geometry of the shield can is also taken into account. In the presence of multiple sources, near field scanning can be performed focusing on a specific source to measure E- and H- fields required for equivalent dipole moments extraction. Tangential E- and H- fields measured on the near field plane are related to equivalent dipole moments by:

$$F_n = T_{nk} X_k \tag{9}$$

The equivalent dipole moments matrix (X_k) is calculated by applying the linear least square method.

$$X_k = \left[T'_{nk} T_{nk} \right]^{-1} T'_{nk} F_n \tag{10}$$

where, T'_{nk} represents the conjugate transpose of T_{nk} matrix and F_n represents tangential E- and H- fields [9]. Using the calculated X_k values, the shielded source can be replaced by

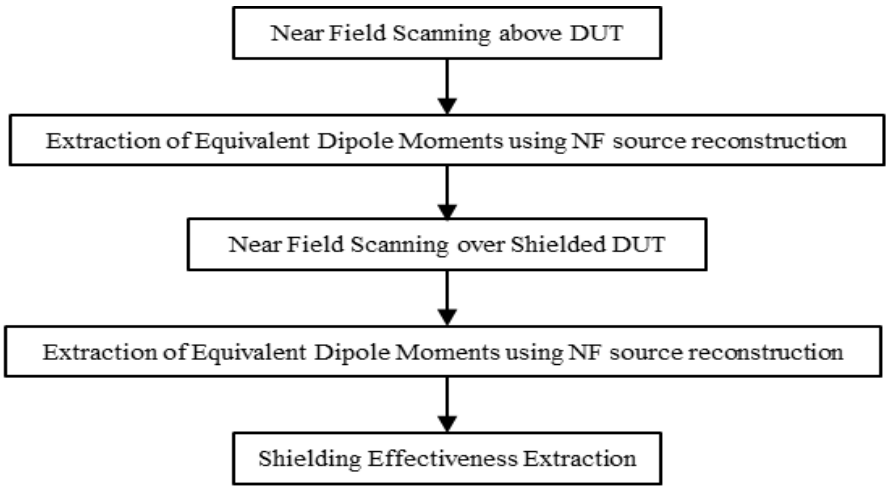

Figure 8. Workflow for nearfield scanning based shielding effectiveness extraction.

an equivalent electric and magnetic dipole moments. Workflow for extracting SE using near field scanning is given in Figure 8.

In order for the proposed SE extraction method to work, an assumption is made: the shielded source can be modelled using a single dipole moment. For example, applying near field source reconstruction method on the near field patterns shown in Figure 7(a), a shielded M_y dipole can be modelled using a single equivalent M_x dipole. The dipole moment of equivalent M_x dipole will reflect the impact of geometry of the shielding can and equivalent source transformation. However, depending on the emission properties of the source and geometrical design of the shielding can, it might not be possible to model the shielded source with a single dipole moment. This can arise from the fact that near field patterns obtained from the source consist of more than one dipole (e.g. 2 M_x dipoles) or more than one type of dipole (e.g. 1 M_x dipole and 1 M_y dipole). Figure 9 shows near field patterns which do not resemble the near field patterns of a single dipole.

To measure the accuracy with which a near field pattern can be modelled using a single dipole moment, two confidence check parameters are applied in this paper: Least Square Error percentage (LSQ error) [9] and Correlation Coefficient (CC) [19]. Using these parameters, a near field pattern can be distinguished if it is made from a single dipole or multiple dipoles, which helps in improving the confidence level of the near field source reconstruction method to model a source using a single dipole moment. LSQ percentage is defined as:

$$\%Error = \frac{\left\| F_n - \hat{F}_n \right\|}{\left\| F_n \right\|} \times 100 \tag{11}$$

where, F_n represents E- and H- fields from near field scanning over the source and $\hat{F}_n$ represents E- and H- fields generated by the equivalent dipole moment of the source. The least square error percentage represents fitting differences between fields measured by near field scanning over the source and fields generated by the equivalent dipole source.

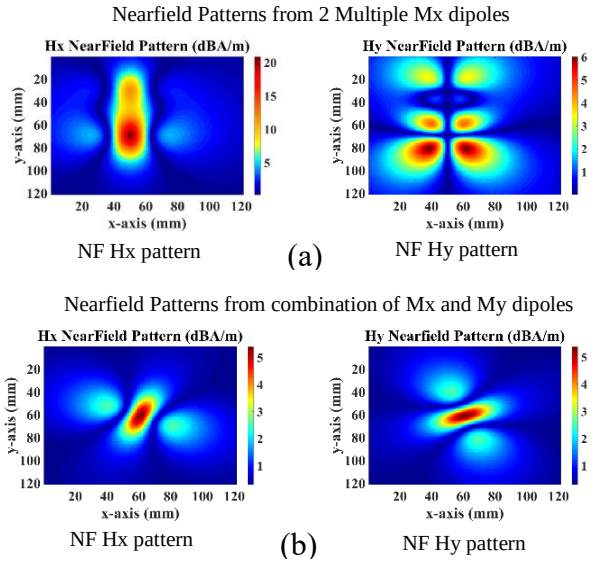

Figure 9. Examples of near field patterns where single dipole model assumption fail. (a) Nearfield pattern from source consisting of 2 M_x dipoles separated vertically. (b) Nearfield patterns from source consisting of 1 M_x dipole and 1 M_y dipole.

The lower the least square error percentage, the better the fitting between the input and reconstructed near field patterns will be and the calculated value of the equivalent dipole moment will be more accurate.

Correlation coefficient (CC) is defined as:

$$r = \frac{\sum_m \sum_n \left(A_{mn} - \bar{A}\right)\left(B_{mn} - \bar{B}\right)}{\sqrt{\left(\sum_m \sum_n \left(A_{mn} - \bar{A}\right)^2 \cdot \left(\sum_m \sum_n \left(B_{mn} - \bar{B}\right)^2\right)\right)}} \tag{12}$$

where, $\bar{A}$ represents mean of values of A and $\bar{B}$ represents mean of values of B. m,n are the dimensions of datasets A and B. Shape vectors of a near field pattern are used as the dataset for correlation coefficient calculation. Shape vectors are extracted by using the contours/shape of a pattern. Correlation coefficient between two near field patterns gives a quantitative number representing the similarity of two patterns based on their shape. Patterns which have similar shape signature will have a correlation coefficient very close to 1. This allows for distinguishing two near field patterns based on their shape. For extraction of equivalent dipole moments using the near field source reconstruction method, near field patterns generated by a source are used as input.

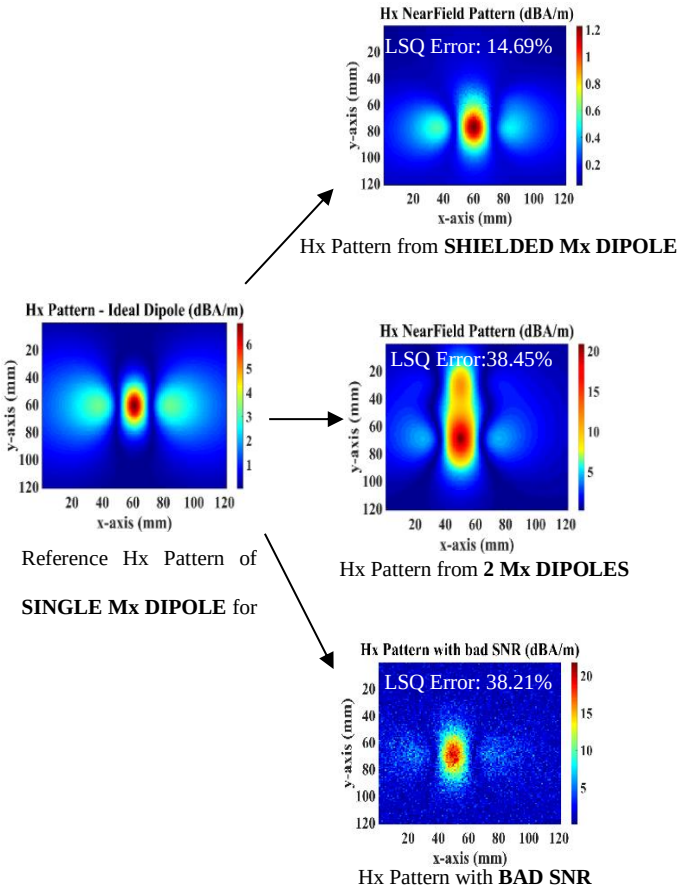

Figure 10. Application of LSQ error for distinguishing near field patterns.

Looking at a near field pattern, one can understand the shape of the pattern and intuitively guess if it is possible to model the source using a single dipole moment or not. LSQ error criteria quantifies the intuition and represents it with an appropriate number. Lower LSQ error percentage implies the source can be modelled with great accuracy using a single dipole moment. Application of LSQ error is illustrated in Figure 10. The H_x near field pattern generated from a shielded M_x dipole, 2 M_x dipoles, and a pattern with bad signal-to-noise ratio are differentiated based on LSQ error percentage. H_x pattern from a single dipole is used as a reference for calculating LSQ error. The near field pattern from a shielded M_x dipole gives an LSQ error of 14.69%, whereas the near field pattern from 2 M_x dipoles gives an LSQ error of 38.45%. This means the shielded M_x dipole source can be modelled more accurately using a single equivalent dipole moment than a source with 2 M_x dipoles.

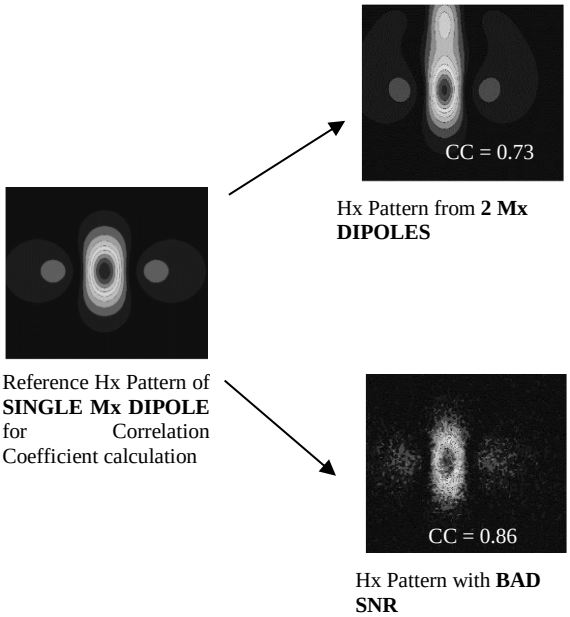

Figure 11. Application of Correlation Coefficient (CC) for distinguishing near field patterns.

For performing any measurement, signal-to-noise ratio (SNR) is one of the important measurement parameters. Having a good SNR is always desirable and enables the measurement of weak signals. However, it is not always possible to have a good SNR. For near field scanning, SNR and number of points in the scan area determine the resolution of the measured near field pattern. In Figure 10, one can see that a H_x pattern with a bad SNR matches more closely with the reference H_x pattern. However, the LSQ error percentage between the H_x pattern from 2 M_x dipoles and the H_x pattern with a bad SNR is not able to distinguish which pattern is better suited for the near field source reconstruction method. Using correlation coefficient, it is possible to differentiate the H_x pattern from 2 M_x dipoles and the H_x pattern with a bad SNR on the basis of shape vectors. Figure 13 shows the application of correlation coefficient on the aforementioned H_x near field patterns.

For calculation of correlation coefficient, the near field patterns shown in Figure 10 are represented based on their shape vectors. Shape vectors contain information about the contours/signature of a pattern. Correlation coefficient represents the similarity of the shape of a near field pattern with the reference pattern. For example, in Figure 11, the H_x pattern from 2 M_x dipoles has a correlation coefficient of 0.73, whereas the H_x pattern with a bad SNR has a correlation coefficient of 0.86. This means, in terms of the shape of the near field pattern, the H_x pattern with a bad SNR matches more closely with the reference H_x pattern. Thus, even though LSQ error for the H_x pattern from 2 M_x dipoles and the H_x pattern with a bad SNR were similar, correlation coefficient showed that the source with a bad SNR near field pattern can be modelled more accurately with a single dipole moment using the near field source reconstruction method. By comparing the near field patterns

with LSQ error and correlation coefficient, one can improve the confidence level of the near field source reconstruction method in modelling a source using a single equivalent dipole moment. Near field patterns generated by multiple dipoles can be modelled with a single dipole moment using a different approach.

If a source has multiple dipoles, then, moving away from the source, the multiple dipoles tend to converge into a single dipole with a net dipole moment value based on the phase relationship between the individual dipoles.

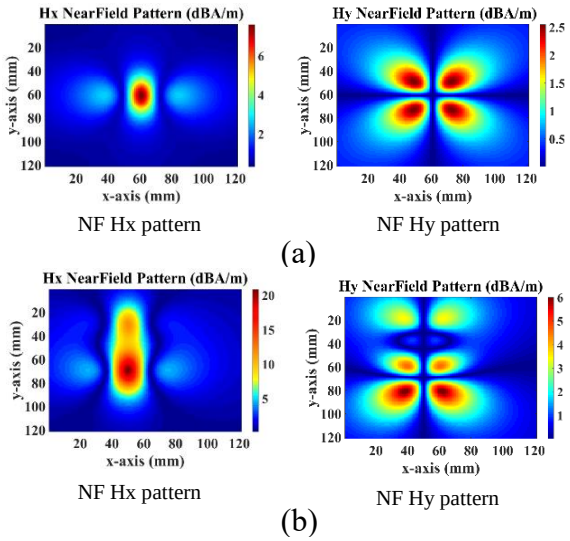

Figure 12: Nearfield patterns at scan height of 10mm. (a) From single M_x dipole. (b) From 2 M_x dipoles

The converged dipole moments retain the location of the dominant dipole among the multiple dipoles. By measuring near field patterns at a height where the dipoles converge, it is possible to model the source with multiple dipoles as a single equivalent dipole. For example, Figure 12 shows the near field pattern generated by a single M_x dipole and 2 M_x dipoles at a scan height of 10mm. At this height, the near field pattern from the

source with multiple dipoles clearly shows the presence of 2 M_x dipoles. By gradually increasing the height of near field scanning plane, 2 M_x dipoles begin to converge into a single M_x dipole. Figure 13 shows the near field patterns generated from a single M_x dipole and the converged M_x dipoles at a scan height of 65 mm. Comparison of the H_x and H_y near field patterns illustrated in Figure 13 shows that the patterns approximately match with each other.

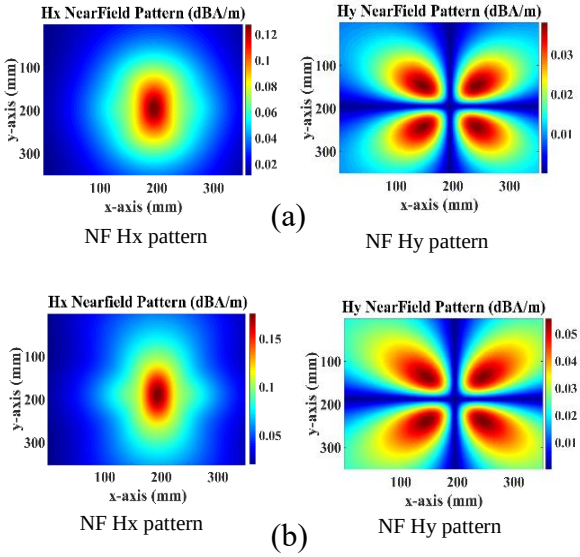

Figure 13: Nearfield patterns at scan height of 65mm. (a) From single M_x dipole. (b) From 2 M_x dipoles

The accuracy with which 2 M_x dipoles source can be modelled using a single M_x dipole moment can be analyzed by calculating LSQ error and correlation coefficient (CC). Table 1 shows the value of the confidence check parameters calculated between the H_x near field patterns illustrated in Figure 12 and Figure 13, respectively. At a scan height of 65mm, LSQ error has reduced by almost 80% and CC has become very close to 1. This proves that by using the near field patterns at a scan height of 65mm, one can model the

source with 2 M_x dipoles as a single equivalent M_x dipole with high confidence by application of the near field source reconstruction method. Single dipole representation for multiple dipoles allows one to extract SE of a metallic can which is meant for shielding two or more sources simultaneously. This would be of great significance in real products where several potential sources are present and shielding cans are employed for suppressing interference.

Table 1. LSQ error and CC comparison between H_x patterns from single M_x dipole and 2 M_x dipoles at scan height of 10mm and 65mm

	NF Scan Height: 10mm	NF Scan Height: 65mm
LSQ Error %	38.45	7.43
CC	0.73	0.94

4. VALIDATION OF EXTRACTED SHIELDING EFFECTIVENESS

A magnetic dipole pointing in the x direction (M_x dipole) representing an active IC is used as an excitation source for calculating SE of shielding cans. SE is calculated for two different models of shielding cans: model A and model B. Both are practical shielding cans used for suppression of RFI in circuit boards of mobile devices. Voltage coupled on a 2.4 GHz PIFA antenna with a shielded source is estimated using simulation and the analytical equations discussed in Sections 2 and 3. Correlation between the simulated and calculated coupled voltage is used to validate the proposed SE extraction method. The simulation model for calculating coupled voltage and extracting SE from shielding can model A is shown in Figure 3. Strength of the excitation source, M_x dipole, is kept as 1 Vm

and the frequency range of interest is from 500 MHz – 6 GHz. Figure 14(a) shows the variation of SE calculated using (1) for shield can model A over the frequency range of interest. It is worth noting that the extracted value of SE_{MxMx} is varying from 15.2 dB – 14 dB over the frequency range of interest.

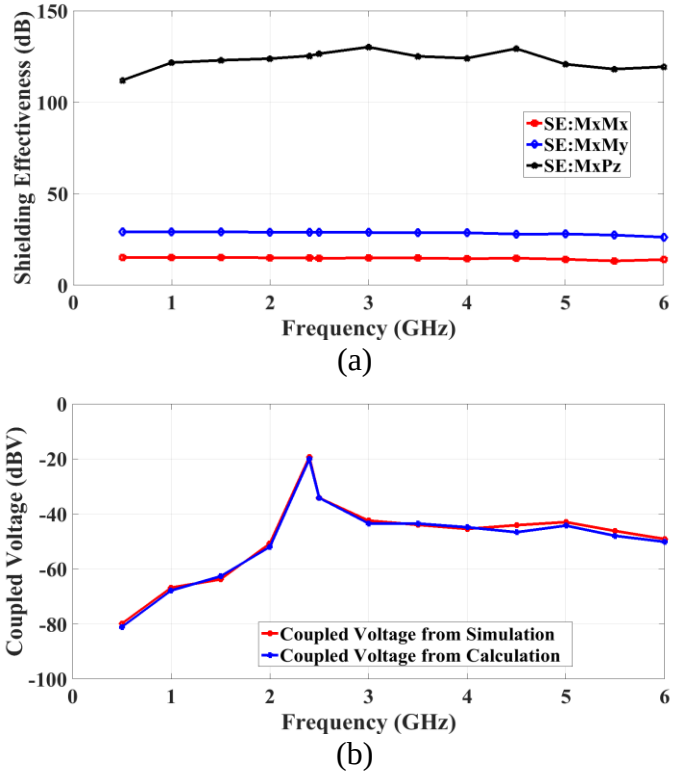

Figure 14. Extracted values for shielding can model A with M_x source excitation. (a) Extracted SE. (b) Coupled voltage validation.

SE values for SE_{MxMy} and SE_{MxPz} are higher than SE values for SE_{MxMx} over the entire frequency range. SE_{MxMy} and SE_{MxPz} represent SE values for the parasitic dipoles created from the shielded M_x dipole. The strength of parasitic dipoles is usually very weak compared to the source M_x dipole. Therefore, the extracted SE value for parasitic dipoles is higher than the extracted SE value of the source dipole. Calculated value of SE will be

accurate only if the equivalent single dipole, representing the shielded M_x source, is extracted correctly using the near field source reconstruction method. The confidence level of the equivalent dipole moment is analyzed by calculating LSQ error and CC as mentioned in Section 3. Table 2 shows calculated values of LSQ error and CC in the frequency range of 500 MHz – 6 GHz.

Table 2. LSQ Error and CC values calculated for shield can model A with M_x source excitation

Frequency (GHz)	LSQ Error %	CC
0.5	14.68	0.89
1	14.29	0.86
1.5	14.94	0.89
2	14.48	0.88
2.4	11.12	0.87
2.5	13.79	0.88
3	13.51	0.89
3.5	13.49	0.85
4	11.45	0.84
4.5	19.48	0.78
5	14.12	0.83
5.5	18.88	0.80
6	15.21	0.84

From Table 2, it is evident that LSQ error is less than 20% at all frequencies and CC is close to 1. This means, the equivalent single dipole representing the shielded M_x source is accurately extracted using the near field source reconstruction method. In other words, the extracted SE is correct. The threshold value for the confidence check parameters can be set based on tolerable error between calculated and simulated coupled voltage from the shielded M_x dipole. Variation of coupled voltage from the shielded M_x dipole over the frequency range of 500 MHz – 6 GHz is shown in Figure 14(b). Simulated coupled voltage

is calculated as mentioned in Section 2, whereas calculated coupled voltage is obtained using (8). The error between simulated and calculated coupled voltage is less than 1 dB. This difference of 1 dB arises due to the fact that (1) does not consider the contribution of multiple reflections between the electrically small source, M_x dipole, and the shielding can model A to the extracted SE.

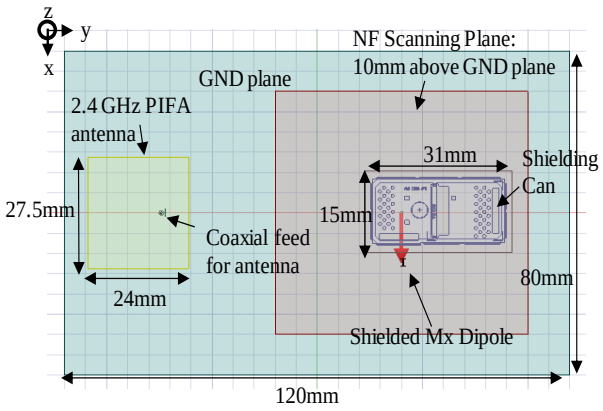

Figure 15. Simulation model for estimating RFI and SE for shielding can model B with M_x source excitation.

The simulation model for estimating coupled voltage and extracting SE from shielding can model B is shown in Figure 15, followed by the extracted SE curve shown in Figure 16(a) and the coupled voltage correlation in Figure 16(b). Extracted SE_{MxMx} for shielding can model B varies from 15 dB – 10.8 dB over the frequency range of interest. As expected, the SE values for the parasitic dipoles (SE_{MxPz} and SE_{MxMy}) are higher than the SE value for the source M_x dipole. The error between simulated and calculated coupled voltage is less than 0.5 dB. Calculated LSQ error was less than 15% for most of the frequencies and CC was higher than 0.90. The error of 0.5 dB between simulated and

calculated coupled voltage could be due to unaccounted multiple reflections between the source dipole and the shielding can.

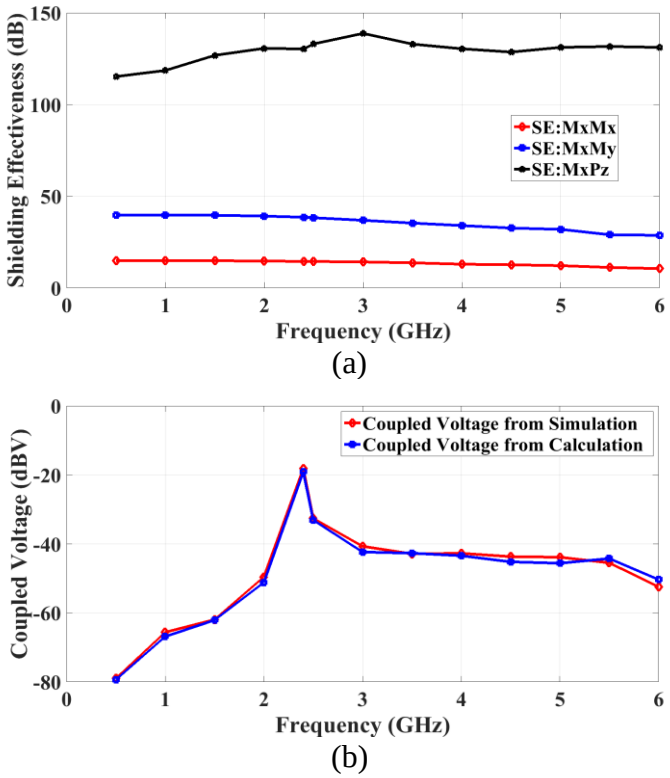

Figure 16. Extracted values for shielding can model B. (a) Extracted SE with M_x source excitation. (b) Coupled voltage validation with M_x source excitation.

The proposed SE extraction method is also applied in the case of equivalent source transformation. Equivalent source transformation happens due to the presence of slots, apertures, castellated edges, and dimensions of the shielding can. The near field patterns shown in Figure 7(a) provide an example of equivalent source transformation. These near field patterns are generated by an M_y dipole source shielded with shielding can model A. The design and geometry of the simulation model used for calculating coupled voltage and extracting SE for the shielded M_y dipole is same as in Figure 3, with the exception that the

excitation source is an M_y dipole instead of an M_x dipole. The strength of the M_y dipole is kept as 1 Vm and simulation is performed over the frequency range of 500 MHz – 6 GHz. Based on the near field patterns shown in Figure 7, the shielded M_y dipole undergoes equivalent source transformation and starts acting as an M_x dipole. SE extracted using (1) for shielding can model A with an M_y source excitation is shown in Figure 17(a). The SE value for SE_{MxMx} is approximately 24.5 dB in the frequency range of 500 MHz – 6 GHz. Correlation between calculated and simulated coupled voltage is shown in Figure 17(b). The error between calculated and simulated voltage is within 1.5 dB until 4 GHz. At 4.5 GHz, the error is about 3 dB and at 5.5 GHz and 6 GHz, there is approximately 8 dB difference between the calculated and the simulated coupled voltage.

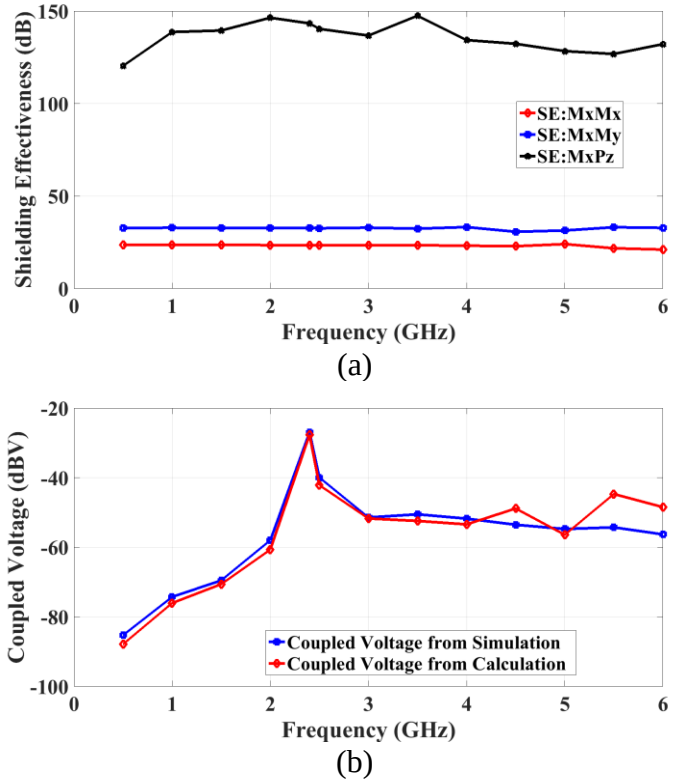

Figure 17. Extracted values for shielding can model A with M_y source excitation. (a) Extracted SE. (b) Coupled voltage validation.

Table 3. LSQ Error and CC values calculated for shield can model A with M_y source excitation

Frequency (GHz)	LSQ Error %	CC
0.5	15.05	0.87
1	15.08	0.86
1.5	14.87	0.89
2	14.47	0.84
2.4	10.54	0.85
2.5	13.44	0.89
3	12.35	0.87
3.5	11.87	0.85
4	11.83	0.84
4.5	17.48	0.77
5	12.92	0.83
5.5	19.77	0.65
6	14.36	0.70

At frequencies where the error is higher than 1.5 dB, the near field pattern from the shielded M_y dipole no longer resembles the near field pattern of a single M_x dipole. This is displayed by a higher LSQ error and lower CC. Table 3 shows the calculated values of the confidence check parameters for SE extraction from the equivalent source transformation scenario. It is worth mentioning that the extracted SE values obtained from shield can model A with M_x and M_y dipoles as excitation sources have a difference of approximately 10 dB. This is because shield model A is not symmetrical and there are a different number of slots present with respect of the direction of the dipole source excitation. Furthermore, there are multiple reflections between the electrically small M_y source and shielding can model A which will also induce error in SE extraction.

5. CONCLUSION

A method to extract shielding effectiveness of board level shielding cans using near field scanning is illustrated. The shielded source is modelled in terms of equivalent dipole moments using a near field source reconstruction method. Shielding effectiveness is defined as the ratio of the dipole moment of the original source to the dipole moment of the equivalent source. LSQ error and correlation coefficient are applied to improve the confidence level in equivalent dipole moment source. Using the calculated SE, an analytical equation is derived to estimate the coupled voltage on a PIFA antenna from a shielded source. The proposed method is validated by correlating the coupled voltage obtained from simulation and the derived analytical equation. The phenomenon of equivalent source transformation due to geometrical design of a shielding can is shown, and shielding effectiveness is extracted successfully. Application of the proposed method on two practical shielding cans is successfully demonstrated and validated.

REFERENCES

[1] F. Vanhee, B. Vanhee, J. Catrysse, H. Yuhui, and A. Marvin, “Proposed methods to measure the shielding performance of PCB level enclosures,” in *Proc. Int. Symp. Electromagn. Compat.*, Kyoto, Japan, 2009.

[2] C. R. Paul, “Shielding” in *Introduction to Electromagnetic Compatibility*, 2nd ed. New York, Wiley, 2006.

[3] L. Gao, X. C. Wei, Y. T. Huang, B. Li, Y. F. Shu, “Analysis of Near-Field Shielding Effectiveness for the SiP Module*,” IEEE Trans. Electromagn. Compat.*, vol. 60, no. 1, pp. 288-291, 2018.

[4] J. Kim and H. H. Park, “A novel IC-stripline design for near-field shielding measurement of on-board metallic cans,” *IEEE Trans. Electromagn. Compat.*, vol. 59, no. 2, pp. 710-716, Apr. 2017.

[5] C. A. Balanis, ‘‘Aperture Antennas’’ in *Antenna Theory Analysis and Design,* 4th ed. New York, Wiley, 2016.

[6] C. Hwang, J. D. Lim, G. Y. Cho, H. B. Park and H. H. Park, “A Novel Shielding Effectiveness Matrix of Small Shielding Cans Based on Equivalent Dipole Moments for Radio-Frequency Interference Analysis,” *IEEE Trans. Electromagn. Compat.*, vol. 58, no. 3, pp. 766-775, June 2016.

[7] P. Wilson, “On correlating TEM cell and OATS emission measurements,” *IEEE Trans. Electromagn. Compat.*, vol. 37, no. 1, pp. 1–16, Feb. 1995.

[8] L. Li et al., "Radiation Noise Source Modeling and Application in Near-Field Coupling Estimation", *IEEE Trans. Electromagn. Compat.*, vol. 58, no. 4, pp. 1314-1321, 2016.

[9] Z. Yu, J. A. Mix, S. Sajuyigbe, K. P. Slattery, and J. Fan, “An improved dipole-moment model based on near-field scanning for characterizing near-field coupling and far-field radiation from an IC,” *IEEE Trans. Electromagn. Compat.*, vol. 55, no. 1, pp. 97–108, Feb. 2013.

[10] Ansys HFSS. [Online]. Available: www.ansys.com.

[11] S. Lee, Y. Zhong, Q. Huang, T. Enomoto, S. Seto, K. Araki, J. Fan and C. Hwang, “Analytical Intra-System EMI Model using Dipole Moments and Reciprocity,” in *Asia-Pacific Int. Symp. Electromagn. Compat.*, Suntec City, Singapore, 2018.

[12] Q. Huang, T. Enomoto, S. Seto, K. Araki, J. Fan and C. Hwang, “Accurate and Fast RFI Prediction based on Dipole Moment Sources and Reciprocity” *Designcon 2018*, Santa Clara, CA, Jan. 30-Feb. 1, 2018.

[13] Q. Huang, Y. Zhong, C. Hwang, J. Fan, J. Rajagopalan, D. Pai, C. Chen, and A. Gaikwad, “Desense prediction and mitigation from DDR noise source,” in *Proc. IEEE Int. Symp. Electromagn. Compat.*, Jul. 2018, pp. 139-144.

[14] Q. Huang, F. Zhang, T. Enomoto, J. Maeshima, K. Araki and C. Hwang, "Physics-based dipole moment source reconstruction for RFI on a practical cellphone", in IEEE Transactions on Electromagnetic Compatibility, vol. 59, no. 6, pp. 1693-1700, Dec. 2017.

[15] Y. Sun, H. Lin, B. Tseng, D. Pommerenke and C. Hwang, "Mechanism and Validation of USB 3.0 Connector Caused Radio Frequency Interference," in *IEEE Transactions on Electromagnetic Compatibility*.

[16] C. A. Balanis, ‘‘Electromagnetic Theorems and Principles’’ in *Advanced Engineering Electromagnetics,* 2nd ed.New York, Wiley, 2012.

[17] Q. Huang, T. Enomoto, S. Seto, K. Araki, J. Fan, and C. Hwang, “A Transfer Function Based Calculation Method for Radio Frequency Interference” accepted to *IEEE Trans. on Electromagnetic Compatibility.*

[18] S. Pan, J. Kim, S. Kim, J. Park, H. Oh, and J. Fan, “An equivalent three dipole model for IC radiated emissions based on TEM cell measurements,” in *Proc. IEEE Int. Symp. Electromagn. Compat.*, Fort Lauderdale, FL, USA, 2010, pp. 652–656.

[19] L. Sheugh and S. H. Alizadeh, "A note on pearson correlation coefficient as a metric of similarity in recommender system," *2015 AI & Robotics (IRANOPEN)*, Qazvin, 2015, pp. 1-6.

[20] H. Yuhui and A. Marvin, “An investigation of the shielding performance of PCB-level enclosures using a reverberation chamber,” in *Proc. IEEE Int. Symp. Electromagn. Compat.*, Honolulu, HI, USA, 2007.

SECTION

2. MEASUREMENT VALIDATION OF NEAR FIELD SCANNING BASED SHIELDING EFFECTIVENESS EXTRACTION METHOD

A test board was designed to validate the near field scanning based shielding effectiveness extraction method. The test board consists of an inverter circuit, input and output ports of inverter, a 796 MHz PIFA antenna and footprints of shielding cans. Figure 2.1 shows the designed test board.

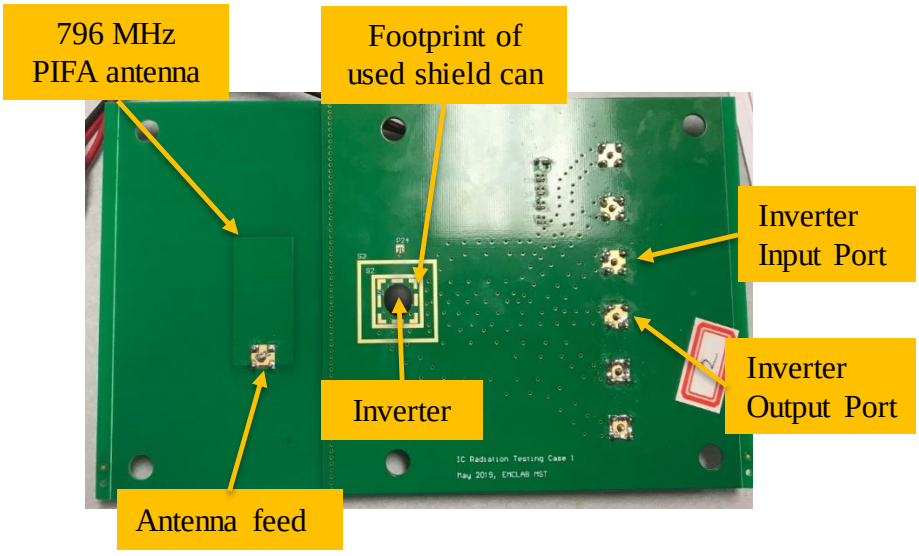

Figure 2.1. Top view of the test board.

A sinusoidal signal with DC offset of 900 mV and peak-to-peak voltage of 1.8 V is fed as input to the inverter using an RF signal generator. Output signal from the inverter is a non-square wave, comprising of fundamental frequency of input sinusoid signal and its higher order harmonics. A real time oscilloscope is used to measure the output from the

inverter. Figure 2.2 shows the time domain and frequency domain signals with input sinusoid frequency of 400 MHz, measured at the output port of the inverter.

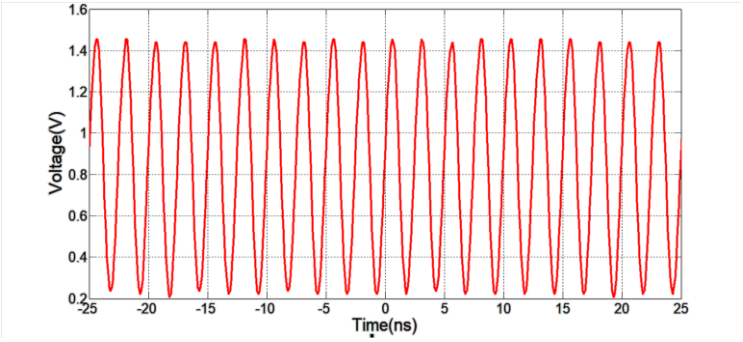

(a)

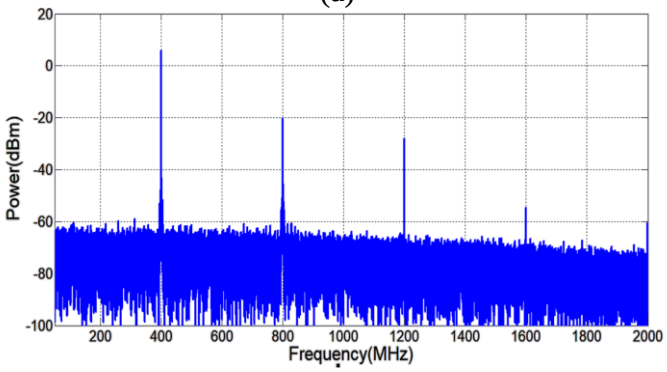

(b)

Figure 2.2. Output signal from inverter. (a) In time domain (b) In frequency domain.

Using near field scanning, first the equivalent dipole moments corresponding to inverter are extracted, followed by extraction of equivalent dipole moments from shielded inverter. Near field source reconstruction method is applied for extraction of equivalent dipole moments from unshielded and shielded inverter. Geometrical and on-board placement details of used shielding can are given in Figure 2.3. Height of near field scan plane is set as 5 mm above the shielding can and frequency range for measurement is from 700 MHz – 900 MHz. Figure 2.4 shows the measurement setup for near field scanning over

shielded inverter. Equivalent dipole moments extracted using measured near field data are used to calculate shielding effectiveness of the shielding can using (1).

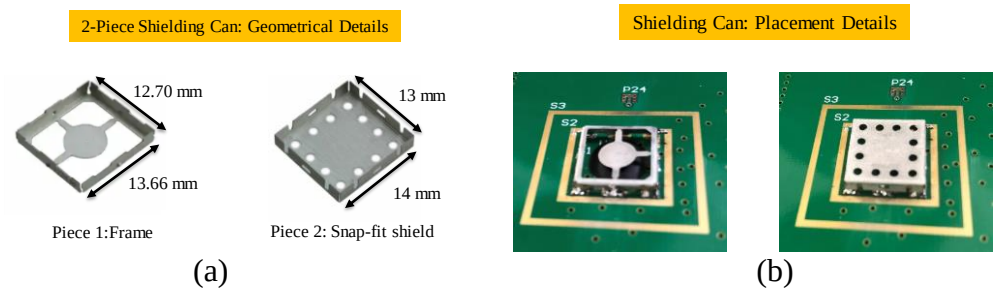

Figure 2.3. Dimensions and on-board placement of shielding can.

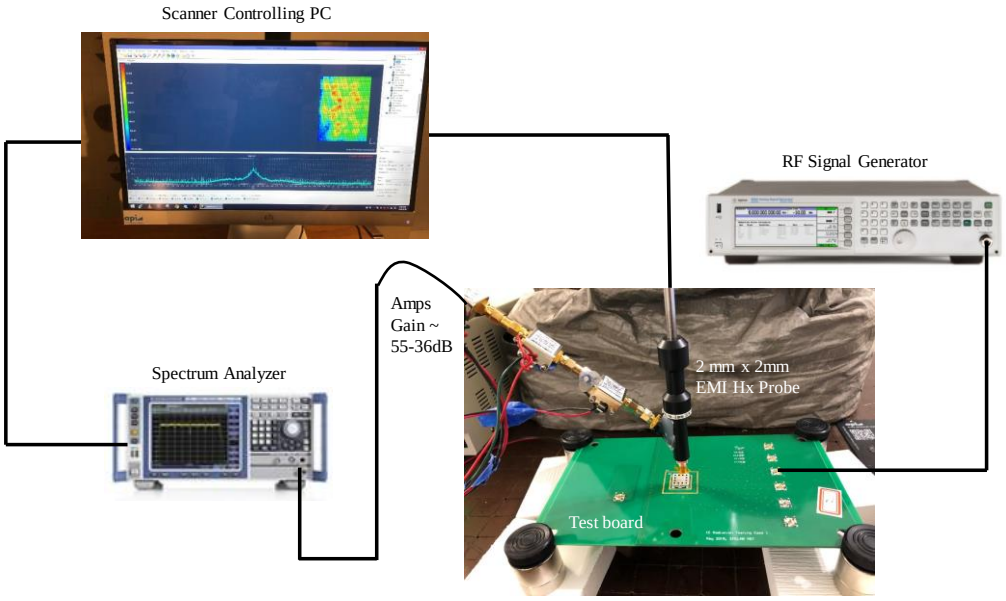

Figure 2.4. Near field scanning measurement setup for shielded inverter.

Coupled voltage from inverter and shielded inverter circuit is measured at the feed of 796 MHz PIFA antenna for the frequency range of interest. Using the extracted shielding effectiveness, coupled voltage from shielded source to PIFA antenna is calculated using (8). Extracted shielding effectiveness for used shielding can is shown in Figure 2.5(a),

followed by Figure 2.5(b) showing correlation between measured and calculated coupled voltage. Correlation between calculated and measured coupled voltage is within 5 dB.

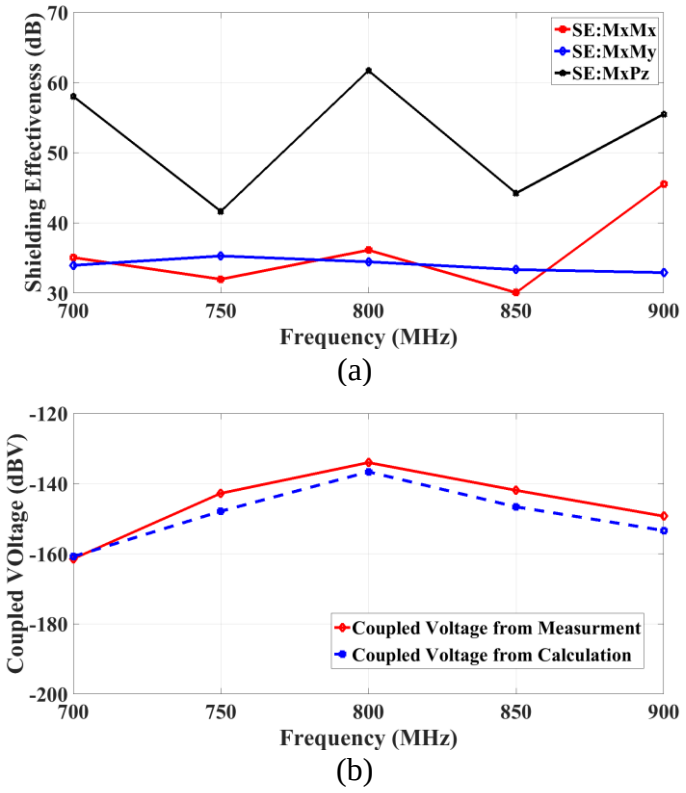

Figure 2.5. Extracted values for shielding can. (a) Extracted SE with M_x source excitation. (b) Coupled voltage validation with M_x source excitation.

Maximum voltage is coupled at close to resonant frequency of PIFA antenna i.e. at 800 MHz. 5 dB error between measured and calculated coupled voltage is due to lack of signal-to-noise ratio at measurement frequencies, presence of unintentional radiation source near the near field scanner and modification in the emission characteristics of the source due to geometry and design of shielding can. By applying the confidence check parameters, accuracy of near field pattern to be modelled using equivalent dipole moments is analyzed. The more accurately a shielded source can be modelled using equivalent dipole

moments, better will be the correlation between calculated and measured coupled voltage. Values of confidence check parameters given in Table 2.1. LSQ error is higher and correlation coefficient is lower for frequencies which have higher relative error between calculated and simulated coupled voltage. By increasing the resolution of near field scan, improving the signal-to-noise ratio and suppressing any unintentional source present in the vicinity of test board, the correlation between calculated and measured coupled voltage can be improved even further.

Table 2.1. Confidence check parameters for shielded inverter

Frequency (MHz)	LSQ Error %	CC
700	53.84	0.75
750	60.16	0.71
800	50.46	0.80
850	57.36	0.73
900	68.29	0.68

3. SUMMARY AND CONCLUSIONS

Shielding cans are critical for suppression of radio frequency interference and preventing radio receiver desensitization issues in modern electronic devices. Having a well-defined method to calculate near field shielding effectiveness is important for estimating the suppression of radio frequency interference using a shielding enclosure. Extraction of near field shielding effectiveness for two practical shielding cans by application of developed method is successfully demonstrated and validated in full wave 3D simulations. Equivalent source transformation is taken into account by using the near field data for calculating shielding effectiveness. Shielding effectiveness is defined in terms of equivalent dipole moments. Application of LSQ error and correlation coefficient to measure accuracy of equivalent dipole moments is usefully illustrated. Using the developed method, near field shielding effectiveness can be obtained for shielding cans used in practical electronic devices. Extracting equivalent dipole moments allows for calculation of shielding effectiveness of shielding can meant for shielding more than one on-board component. Measurement validation of developed method was demonstrated by using a test board. Measurement challenges such as insufficient signal-to-noise ratio and presence of unintentional radiation source resulted in poor measurement results. Improvement of signal-to noise ratio and suppression of unintentional radiation source can improve measurements results significantly.

BIBLIOGRAPHY

[1] C. R. Paul, “Shielding” in *Introduction to Electromagnetic Compatibility*, 2nd ed.New York, Wiley, 2006.

VITA

Harsh Shrivastav received B. TECH degree in Electrical and Electronics Engineering from the SRM University, India in 2015. He started his M.S. degree in Missouri University of Science and Technology, Rolla, MO, USA in August 2016. In May 2017, he started working with electromagnetic compatibility laboratory. His research interests included: RF interference investigation and mitigation for on-board RF receivers, RF circuit design, EMC testing, grounding and shielding techniques to improve electromagnetic compatibility. He received his M.S. degree in Electrical Engineering from Missouri University of Science and Technology, Rolla, MO, USA in December 2019.